

CHAPTER 25

DYNAMICS OF WIND IN THE VICINITY OF PROGRESSIVE WAVES

Omar H. Shemdin
Acting Assistant Professor, Stanford University
Stanford, California

AND

En Yun Hsu
Associate Professor, Stanford University
Stanford, California

ABSTRACT

This paper presents a fundamental study of the dynamics of wind in the vicinity of progressive water waves. The normal pressure distribution and the structure of the velocity profile immediately above progressive water waves are investigated.

A wind-wave facility 115 feet long, 74½ inches high, and 35½ inches wide is used which is equipped with an oscillating-plate wave generator. Velocities up to 80 fps can be obtained at a nominal water depth of 3 feet.

An oscillating device (or wave follower) was designed and built, on which a pressure sensor could be mounted and could be held at a fixed distance (within ¼ inch) above progressive water waves at all times.

The results indicate that a pressure shift does exist as predicted by Miles [1957] within the assumptions of the theory. Furthermore, the results demonstrate clearly the importance of using a pressure sensor which follows the water surface in obtaining meaningful pressures at the air-water interface. Mean velocity profiles with and without mechanically-generated waves were obtained. Contrary to what is normally assumed, the results indicate that the boundary layer in the vicinity of water waves is affected by the presence of waves.

INTRODUCTION

The interaction between wind and sea results in the generation of water waves by a complex process which, for the sake of simplicity, can be visualized as follows. An air stream, blowing over a body of water that is initially at rest, generates surface currents in the water. This is a result of the shear action exerted by the wind. When the wind exceeds a certain minimum speed, the water surface becomes unstable and small wavelets begin to appear. These wavelets propagate in the general down-wind direction. The wavelets grow in amplitude and increase in length as they propagate and their rate of growth is highly dependent on the characteristics of the

boundary layer profile in the wind just above the water. The appearance of the waves, however, changes the boundary conditions at the air-water interface and thus produces a change in the structure of the wind profile. The latter, in turn, influences the growth of the waves. This process can be best thought of as one of cause and effect between two fluid systems which are coupled together. At the present time, neither the degree of coupling nor the governing mechanisms in either fluid can be regarded as known.

The growth of waves is limited by dissipating mechanisms such as the breaking of waves and viscous action in the water. Indeed, the net energy input into the water from air through the interface is identical to the sum of that part of the energy contributing to the growth of waves and that part which is dissipated. Furthermore, waves will grow if the energy extracted from the wind exceeds that which is dissipated, while a state of equilibrium will result when this energy is equal to that which is dissipated by the waves' motion. Finally, if the energy supplied is less than the energy lost as a result of the viscous action in the water, the waves will decrease in size until a new equilibrium is reached. Therefore, a complete understanding of the growth of waves necessarily requires the understanding of the dissipating mechanisms in water as well.

BACKGROUND

Several theoretical investigations have been made to explain the phenomenon of wind-wave generation. The first attempt was made by Kelvin and Helmholtz [see Lamb, 1945] employing a mathematical model based on the inviscid motion of two fluids moving at different velocities and separated by a surface of discontinuity. The results predicted a minimum speed for the generation of waves which is much greater than that observed in nature. Jeffreys [1924, 1925] advanced a semi-empirical theory that introduced the concept of sheltering based on an assumed distribution of pressure, which is in phase with the wave slope, such that a higher pressure is exerted on the windward side than the leeward side of a wave crest. The theory requires the empirical determination of a sheltering coefficient (a nondimensional pressure coefficient) from ocean data which has been estimated to be 0.3.

Experimental studies aimed at verifying the sheltering hypothesis of Jeffreys have been made by Stanton et al [1932], Motzfeld [1937], and Larras and Claria [1960]. These investigators measured normal pressures in air streams close to stationary wavy surfaces. Their results indicated sheltering coefficients one order of magnitude smaller than the value predicted by Jeffreys. If these measurements were to hold for progressive water waves, then Jeffreys' model (i.e., normal stresses) would not account for the observed energy transfer from air to water. The major objection, however, which throws doubt on the validity of the above experimental results is that they were all performed on stationary surfaces.

In a critical review of the existing knowledge on wave generation by wind, Ursell [1956] concluded that "the present state of our knowledge is

profoundly unsatisfactory." This seems to have stimulated further interest in this area of research, culminating in a series of papers by Miles [1957, 1959a, 1959b], Phillips [1957], Benjamin [1959], and Lighthill [1962]. Phillips [1957] suggested that the mechanism responsible for the growth of water waves is one of resonance between the water surface and the random pressure fluctuations inherent in a turbulent velocity field. In a discussion of the experimental results obtained by Cox [1958], Phillips conjectured, however, that his theory may be valid in the initial stages of wave growth only. Miles [1957] introduced a new concept of a one-way coupling between an air stream and the water surface over which it blows. Accordingly, air blowing over a wavy water surface causes the waves to grow, but the motion of the wavy surface does not alter the character of an air stream above it. Miles further assumed a mean turbulent velocity profile but neglected both viscosity and turbulent velocity fluctuations. The results indicate that a phase shift exists between the normal pressure distribution along the wave and the wave itself, such that a higher pressure is exerted on the windward side than on the leeward side of a wave crest as shown in Fig. 1. Later, Benjamin and Miles [1959, 1962] included viscosity in the theoretical model and concluded that viscous effects could be very important in certain stages of wave growth. Lighthill viewed the mechanism presented by Miles from the physical standpoint by examining the distribution of vorticity along a wavy surface in the air stream. In a steady-state model, he emphasized the existence of a critical layer in the air stream close to the water surface which, effectively, can be held responsible for the energy transfer from air to water.

Several experimental attempts have been made to verify the newly advanced theories by Cox [1958], Cohen and Hanratty [1965], Hidy and Plate [1965], and Wiegel and Cross [1966] under controlled environment and by Longuet-Higgins [1962] in the ocean. The results have been instrumental in obtaining a qualitative description of the growth of waves, and inferences were made of the validity of the above theories from the measured rates of growth and measurements of pressures in the air. The results, however, leave much to be desired in the way of conclusive verification of the theoretically suggested growth mechanisms and the regimes of flow under which they become efficient in transferring energy from air to water.

A successful experiment measuring the phase shift between the normal pressure and the wavy boundary was made by Zagustin et al [1966] in an experiment in which the water surface was replaced by a flexible wavy surface which moves between guides fixed in space. Water was employed as the fluid medium and was allowed to flow in the direction opposite to that of the moving wavy boundary. Thus a steady-state flow picture was created to simulate wind blowing over small amplitude progressive waves. Pressures were measured along the wavy surface in the critical layer. The results indicated a phase shift between the normal pressure distribution along the wavy boundary and the boundary, and was found to be in close agreement with the theoretical prediction of Miles [1957]. The shift was found to disappear when the moving boundary was brought to rest, at which point the experimental conditions became identical to flow over a fixed wavy boundary.

The shear-flow mechanism proposed by Miles [1957] and Benjamin [1959] and the experiments of Zagustin et al [1966] emphasize the role of a critical layer in the close vicinity of a moving surface as defined in Fig 1. The vorticity in the layer is seen responsible for the phase shift in the normal pressure distribution along the wave. The shift promotes the transfer of energy from air to water. In a turbulent velocity profile the critical layer height is small compared to the wave height. Therefore, the experimental verification of the important role of the critical layer in energy transfer to progressive water waves requires the measurements of very small pressure inside the critical layer, i.e., under unsteady conditions (so that a pressure sensor may be kept close to the moving surface). It was, therefore, the aim of the present investigation to measure, under unsteady conditions, the static pressure distribution inside the critical layer above the surface of two-dimensional progressive water waves under a controlled laboratory environment.

APPARATUS AND PROCEDURE

THE WIND WATER-WAVE FACILITY

The newly constructed wind-wave facility in the Hydraulics Laboratory at Stanford University was used for the experimental study. A detailed description of this facility is given by Hsu (1965). The channel is 115 ft. long, 74½ in. high, and 35½ in. wide. The test section is 85 ft. long and is constructed with glass for photographic recording of waves. The entire channel is enclosed with a set of 5-ft.-long steel, roof-plates at the top of the channel (a typical portion of the test section is shown in Fig. 2). A 5-ft.-long aluminum plate, used for mounting the wave follower and other instruments, is designed to replace conveniently any one of the regular steel-roof cover plates. Consequently, measurements can be made at any distance along the test section.

The wave generator is a horizontal displacement-type oscillating plate. It is driven by a hydraulic power cylinder and controlled by an electro-hydraulic power system, so that the motion of the plate may respond to an arbitrary input electrical signal. Sinusoidal waves, ranging in frequency from 0.2 to 4.0 cps, can be generated. Solitary waves and waves of complex shape can also be generated by the system.

To absorb the energy of the generated waves, a beach is installed at the downstream end of the channel. The beach is made of baskets 12 in high, 24 in. wide, and 36 in. long, filled with stainless steel turnings and placed on wood slats over a steel frame at a slope of 1 to 5. The reflection coefficients of the beach for waves ranging in frequency from 0.6 to 1.2 cps, is found to be less than 10 per cent.

The air intake is located 17 ft. downstream of the mean position of the wave generator plate so that the generated waves become fully established (a horizontal distance three times the water depth is desired) before exposure to the action of wind. The air intake is elbow-shaped

as shown in Fig. 3 and is augmented with three turning vanes inside the elbow, a wire screen, and a 2 in.-wide honeycomb with $\frac{1}{4}$ -in. hexagonal matrix at the inlet to the test section. This is to insure the proper shape of a boundary-layer profile and to minimize the angularity of the incoming flow. The elevation of the elbow-air intake can be adjusted with respect to the channel from up to approximately 12 in. It is normally set at about 6 in. above the free surface for a nominal water depth of 3 ft. A transition plate is installed at the toe of the air intake to insure a smooth transition for air flow into the test section. The transition plate was artificially roughened to create a relatively thick boundary layer. The latter was found necessary to insure critical layer heights in the proper range for experimental measurements.

A suction fan is installed at the downstream end of the channel. The fan is driven by a motor capable of creating a maximum free-stream air velocity of 80 fps at a nominal water depth of 3 ft. The speed of the fan is controlled electronically to ± 1 rpm at all speeds.

MEASUREMENT OF WAVE HEIGHT AND WIND VELOCITY

A capacitance-type gage and a capacitance bridge were used to measure wave heights. The gage frame was made of a U-shape bracket. A Nyclad insulated wire, No. 36 HNC, having an outside diameter of 0.006 in., was used for a sensor. Both ends of the wave-height sensor were cast into Lucite fittings for water proofing and for insulating the sensor from the U-frame on which the sensor is mounted. The capacitance bridge was designed by Dr. A. Miller of Sanborn Instrument Company of Waltham, Massachusetts, for suitable use with Sanborn 958-1100 and 650-1100 series-type recorders. Use was made of a transformer to isolate the bridge from the recorder carrier-amplifier to eliminate ground-loop effects. In the present experiments, the wave gage and capacitance bridge were used satisfactorily with a Sanborn 650-1100 series optical-type recorder. The system was calibrated before and after each run.

The velocity in the air was measured by using a Pitot-static probe in conjunction with a sensitive pressure transducer and a Sanborn 650 optical-type recorder. The $\frac{1}{32}$ in. O.D. Pitot-static probe used is a standard shelf item manufactured by United Sensors and Control Corporation. The pressure transducer used had a full range of ± 1 in. of water (± 0.037 psid) and was manufactured by Pace Instrument Company (model P90 D). A static calibration of the transducer and the recording system was obtained with the use of a Harrison micromanometer. Only mean velocities at each elevation above the mean water level were obtained and both temperature and humidity effects were taken into account when converting dynamic pressure data into velocities.

MEASUREMENT OF STATIC PRESSURE NEAR A PERTURBED SURFACE UNDER UNSTEADY CONDITIONS

The best possible technique for measuring the surface pressures near the interface of a progressive water wave in the wind-wave facility was considered to be that of maintaining a pressure sensor at a small fixed

distance above the changing water surface and at a fixed position along the channel. Three major tasks were to be completed successfully in order to expedite this technique of measuring pressures

1. Designing a mechanical system capable of holding a pressure sensor that can move freely in the vertical direction,
2. Designing an electronic control system to maintain the pressure sensor at a fixed distance above a changing water surface,
3. Recording the pressures sensed under unsteady conditions and determining the content of the record.

The mechanical system of the wave follower - The basic mechanical system was made of a (2 in. O.D., and 1¼ in. I.D.) cylinder fixed to the roof of the channel. Two high-precision ball bushings were inserted at each end of the hollow cylinder, so that a precision-ground hollow cylinder (¾ in. O.D. and 3/8 in. I.D.) can be moved freely between the bushings through the use of an electric motor with a gear and rack system, as shown in Fig. 5. The motor was mounted to a base fastened to the 2 in. cylinder by set screws.

The pressure-sensing system - The pressure-sensing system consisted of two pressure sensors and the Pace differential pressure transducer

The first pressure sensor consisted of a ¾ in. diameter, 1/8 in. thick brass disk with two 0.030 in. side holes at the center. An inter-connecting passage, having a diameter of 0.060 in. along the radial direction of the disk, connected the side holes to a ¼ in. O.D. stainless steel tubing. This tubing acted both as a conduit and support holding the pressure sensor. The conduit was fastened to the lower end of the moving cylinder through the use of a circular flange. From the lower end of the moving cylinder, the pressure was transmitted to one side of the differential pressure transducer through a ¼ in. O.D. tubing which fit inside the inner moving cylinder. The disk shape of the sensor was especially chosen to minimize the effects caused by its own motion. The edge of the pressure-sensor disk was streamlined to avoid flow separation. The pressure sensor is shown in Fig. 5b.

An identical pressure sensor was made to measure the mean-free-stream static pressure and was located at a mean distance of 11 in. below the roof. The static pressure sensor was connected to the other side of the differential pressure transducer as shown in Fig. 5a and c.

The same Pace differential pressure transducer was used for both velocity and pressure measurements. The transducer was mounted on the moving inner cylinder. The positive side of the transducer was connected to the pressure sensor near the interface. The negative side of the transducer was connected to the reference static probe, by a ¼ in. stainless steel tubing which could slide freely through the ¼ in. bore of a ball bushing mounted on the roof plate, as shown in Fig. 5c.

The entire sensing system moved as a unit when the pressure sensor followed the water surface, so that the strenuous pressures caused by the deformation of the tubing could be eliminated. The present scheme was devised after less successful trials in which the transducer was kept fixed in space relative to the moving cylinder. The motion of the transducer produced negligible effects on the pressure measurements, since the Pace transducer was based on the variable-reluctance principle. According to the specifications furnished by the manufacturer, the acceleration sensitivity of the transducer was 0.001 psi per g in the more sensitive direction (normal to the diaphragm). Since the orientation of the transducer diaphragm was parallel to the direction of motion, the motion of the transducer produced no significant effect on the pressure measurements.

The entire sensing system was calibrated for frequency response. The pressure sensor was placed inside a pressure chamber designed and constructed for this purpose, in which the pressure could be varied sinusoidally at a fixed small amplitude and for frequencies ranging from 0.3 to 3.5 cps. The reference static probe was left outside the pressure chamber. The sensing system exhibited instantaneous response for frequencies beyond 3 cps which is well beyond the range of the present investigation.

The electronic controls of the wave follower - The position of the inner-moving cylinder was controlled by an elevation control gage (identical in construction to a wave-height gage) mounted on the lower end of the inner cylinder, as shown in Fig. 5b. The position of the pressure sensor relative to the perturbed water surface was governed by preselecting a fixed capacitance for the partially submerged elevation control gage. Whenever a change in water level occurred, a corresponding change followed in the capacitance of the control gage caused by the changing of its submergence. The electronic control of the wave follower tried to maintain the preselected capacitance of the elevation control gage. Thus, when the water surface elevation rose as a result of a wave disturbance, the elevation control gage sensed the change and consequently the control electronics commanded the motor to move the inner cylinder upward until the original capacitance was restored. The reverse took place when the water surface receded. The above process is shown schematically in Fig. 4.

The position of the inner cylinder, with respect to the instantaneous water surface, was given by a position indicator gage (same in construction as a wave-height gage). This gage was mounted on the inner cylinder adjacent to the elevation control gage, shown in Fig. 5b. The position-indicator gage was no more than a wave-height gage that moved vertically with the inner cylinder. The record obtained from the position-indicator gage reflected the error involved in maintaining the moving cylinder at a fixed distance above the instantaneous water surface (or a record of zero fluctuation from this gage indicated that the moving cylinder was maintained exactly at a fixed distance above the water surface at all times). The wave follower was found to follow, within $\frac{1}{4}$ in., the surface of mechanically generated waves having frequencies as high as 1 cps.

Because the basic objective of this study is to measure surface pressures over pre-existing waves, simultaneous records of wave heights

and surface pressures are desired. For this purpose a wave-height gage was provided with the wave-follower assembly and was mounted on the fixed outer cylinder as shown in Fig. 5c. The procedure followed in obtaining pressure data was to generate the desired mechanical wave and to allow the pressure sensor to follow the water surface at a distance of approximately $\frac{1}{2}$ in. above the water surface. Then with the sensor following the water surface the wind speed was increased in small increments from zero to about 40 fps. At each wind speed the pressure data consisted of simultaneous recordings of 1) the wave profile, 2) surface pressure, and 3) position error of the pressure sensor.

Undesirable high-frequency pressure fluctuations (compared to wave frequency) caused by electrical noise, aerodynamic turbulent fluctuations, and mechanical vibrations of the apparatus were eliminated by externally superposing capacitance on the signal obtained from the pressure transducer. Pressure fluctuations, having frequencies one order of magnitude larger than the wave frequency, could be eliminated without affecting the perturbation pressure resulting from the perturbed water surface. However, the addition of sufficient capacitance, to filter out some undesirable pressure fluctuations inherent in the oscillating system, caused an amplitude reduction and phase lag in the pressure signal. The externally added capacitance on the transducer signal could lead to erroneous results if not accounted for. In the present experiments, this effect was accounted for by 1) calibrating for the amplitude attenuation due to the superposition of external capacitance on the pressure signal, and 2) by adding an identical magnitude of capacitance to the wave height signal whenever capacitance was added to the pressure signal. The latter procedure eliminated any relative electrical phase shift between the pressure and wave height signals when recorded simultaneously. The phase shift due to external capacitance was also determined during the calibration of the sensing system to check the procedure for recording the pressure data. The procedure was found to give proper phase relationship between the pressure and wave height signals when recorded simultaneously.

EXPERIMENTAL RESULTS

The verification of the theoretically proposed mechanisms of energy transfer from air to water requires the investigation of a) the air velocity profile above a perturbed water surface, and b) the measurement of air pressure as close as possible to the interface between air and water. In the present investigation, separate runs were conducted to measure the air velocity profile, and the air pressure distribution at the interface, for each mechanically-generated water wave with a prescribed frequency and amplitude. The perturbation pressure at the interface was measured under two conditions, a) the pressure sensor following the water surface and b) the pressure sensor fixed in space above the crest. Waves having different frequencies and amplitude were investigated. The results obtained for the 0.6 cps mechanically-generated waves only are presented here as a representative sample.

AIR VELOCITY PROFILES

The mean velocity profiles over the 0.6 cps mechanically generated wave were obtained by measuring the average dynamic wind pressure at fixed points in space above the mean water level and plotting the velocity at each point with respect to the mean water level to obtain the velocity profile for each blower speed setting. Profiles were obtained at blower speeds of 40, 60, 80, 100, 140, 160, and 200 rpm consecutively as shown in Fig. 6. The straight lines fitted to the data were by the method of least squares. The measurements were taken at sta 17.5 (or 17.5 ft downstream from the air inlet).

In order to gain some insight into the degree of influence that a water-surface perturbation has on the air velocity distribution, mean-velocity profiles were obtained with and without the presence of a mechanically-generated water wave. The air velocities were measured at station 57.0 which is 57 feet downstream from the air inlet and 28 feet upstream from the air exit. Therefore, it was assumed that the velocity profiles were not influenced by either the inlet or exit conditions. The estimated set-up at this station was found to be 0.5 inches and was taken into account when plotting the mean velocity profiles with respect to the mean water level. The velocity profiles with and without the presence of mechanically-generated waves are presented in Figure 7.

MEASUREMENTS OF PERTURBATION PRESSURES

The basic mechanism responsible for energy transfer from air to water in the theories proposed by Miles (1957) and Benjamin (1959) is that the vorticity inherent in the air-velocity distribution causes a phase shift in the aerodynamic-pressure distribution over the perturbed water surface and consequently promotes energy-transfer from air to water. Furthermore, the above theories suggest that the pressure shift occurs only in a thin layer y_c , above the water-surface defined by $U(y_c) = c$ where c is the speed of the surface wave. Since the critical layer is expected to be small (compared to the wave amplitude) for a turbulent boundary-layer, it is expected that a pressure sensor fixed in space above the crest of a progressive wave will remain outside the critical-layer most of the time under moderate wind speeds. Therefore, in order to verify experimentally the important role played by the critical layer at the air-water interface in energy transfer, the aerodynamic pressure distribution over the wave train was measured with a pressure sensor following the water surface and compared to the aerodynamic pressure measured with the same sensor fixed in space above the crest under the same test conditions. The wave-frequency and wind-speed were carefully chosen in light of the theories proposed by Miles (1957) and Benjamin (1959) to insure a sufficiently thick critical-layer so that the pressure sensor can be maintained inside it when following the water-surface. Original samples of the instantaneous recording of the pressure signal, wave height, and the error associated in keeping the pressure sensor at a fixed distance above the instantaneous water surface are shown in Fig. 8 for the case when the pressure sensor follows a 0.6 cps mechanically-generated wave and for wind velocities 0.0, 5.5, and 9.5 fps.

The direct recordings of pressure clearly indicate periodic variations of the perturbation-pressure with a frequency approximately equal to that of the mechanically-generated wave. The pressure records also show additional random high-frequency fluctuations superimposed on the periodic variation which are attributed to the motion of the pressure-sensing system and the inherent noise in the electronic circuitry. A closer examination of the pressure records with increasing wind speeds, however, reveals a systematic increase in the phase-shift between the pressure signal and the wave profile.

In order to obtain more meaningful data about the perturbation pressure, a "time-averaging" procedure was used to eliminate the high-frequency pressure fluctuations. The procedure followed in the averaging process was a) duplicate the original pressure record on a transparent paper for about three wave-lengths such that the high-frequency fluctuations are eliminated, b) shift the transparent paper over the original record one wave length without changing the lateral position of the transparent paper with respect to the original record, c) duplicate the pressure records at the new position of the transparent paper, and d) repeat the above procedure for as many wave-lengths as available in the total pressure record. In general, three or four duplications of the pressure record over three wave-lengths could be obtained. A least-square sinusoidal fit to the superimposed duplications could be calculated to yield the amplitude and phase angle of the best fit sine curve. The superimposed pressure duplications and the best-fit pressure curves above a 0.6 cps mechanically-generated wave when the pressure sensor is following the water surface and when the pressure sensor is fixed above the crest are shown in Figs 9 and 10 respectively.

DISCUSSION OF RESULTS

MEAN VELOCITY PROFILES

The mean velocity profiles plotted with respect to the mean water level above the 0.6 cps mechanically-generated wave, shown in Fig. 6 can be approximated by a logarithmic distribution, a result that has been suggested by many previous investigators. However, the velocity profiles obtained for the purpose of investigating the influence of waves on the mean velocity profile, shown in Fig. 7, indicate a definite change in the wind velocity profile due to the presence of the mechanically-generated wave. The velocity profile over the water surface disturbed by wind-generated waves only (no mechanically-generated waves) deviates from a logarithmic velocity distribution such that higher velocities are observed closer to the water surface than predicted by a logarithmic fit. The results indicate that while a logarithmic fit may be a reasonable approximation for wind profiles over mechanically-generated waves, such an approximation cannot be applied for wind over wind-generated waves only. This result is interpreted only as an indication that the wind velocity profile depends on the wave characteristics at the air-water interface. Such a result can be important when computing energy input into waves from measured velocity distribution by the use of theoretical results of Miles

[1959]. The latter is sensitive to the shape of the velocity profile at the critical layer height.

AERODYNAMIC PRESSURE OVER THE WATER SURFACE

The pressure sensor following the water surface - The superimposed pressure records at different wind speeds shown in Fig. 9 for the case when the pressure sensor follows the water surface exhibit clearly a change in amplitude and a continuous phase shift in the pressure distribution with respect to the water wave with increasing wind speeds. The phase shift is in the direction necessary for the transfer of energy from air to water (i.e., high pressure on the windward side and low pressure on the leeward side of a wave crest). The content of the pressure records, however, cannot be directly compared with the theoretical predictions of Miles [1957, 1959] since the dynamic effect of the moving pressure sensor is superimposed on the pressure signal and the pressure at the interface is referenced to the pressure in the free stream.

The inviscid theory from a frame of reference fixed in space, predicts a pressure distribution above a sinusoidally perturbed surface which can be given in the following nondimensional form in an infinitely high channel.

$$\frac{p_a}{\rho_a g \eta} = - \left[\frac{U_a}{c} - 1 \right]^2 \exp(-ky)$$

where p_a is the aerodynamic pressure, η is the wave profile with respect to the mean water level, g is the gravitational acceleration, ρ_a is the air density, U_a is wind velocity, c is the wave speed, k is the wave number, and y is the vertical axis which is positive upward. Therefore, the inviscid theory predicts a pressure distribution 180 deg out of phase with the wave at $U_a = 0$ and zero pressure when $U_a = c$.

The pressure record shown in Fig 9 exhibits no perturbation due to the wave at zero wind speed and a perturbation in phase with wave when $U_a \approx c$. The latter is seen to imply that the dynamic effect of the moving probe is equal in magnitude and opposite in phase to the pressure distribution caused by the wave at zero wind speed. Furthermore, the dynamic effect of the moving probe remains unchanged as the wind speed is increased. Therefore, it is concluded that the continuous phase shift observed in Fig. 9 with increasing wind is due to the aerodynamic influence of wind on a perturbed surface and that the dynamic effect need be taken into account only when comparing the above experimental results with the theoretical predictions of Miles [1959].

The pressure sensor fixed in space above the crest - If one examines Fig. 10 carefully in light of the decreasing critical layer thickness (obtained from measured velocity profiles shown in Fig. 6) some added insight can be gained into the role of the critical layer mechanism in bringing about a pressure shift. When $U_a = 0$, the pressure distribution is out of phase with wave as predicted by the inviscid theory (expected to

hold for $U_a = 0$ and $U_a \gg c$). As the wind speed increases and reaches a maximum of about 8.00 fps (phase speed = 7.55 fps), the pressure signal becomes minimum in amplitude (a result which is also consistent with the inviscid theory. When the wind speed is increased slowly to 15.0, however, a pressure signal having the frequency equal to that of the water wave appears and is shifted approximately 75 degrees with respect to the wave. It is interesting to note that at maximum wind velocities between 9.5 and 15.0 fps, the corresponding critical layer thickness is between 5.0 and 1.0 inches, respectively. With the 3.00 inch wave height investigated, this means that when $V_{max} < 15.0$ fps the probe (fixed above the crest) remains inside the critical layer most of the time, while the reference static probe remains outside the critical layer. The measured shift is consistent with Miles' theory. It is worth noting that a possible experimental verification of Miles' theory can be made in this range even with the probe fixed in space. It is emphasized that the above results are consistent with those obtained with the pressure sensor following the water surface.

The pressure records in Fig. 10 show a high degree of irregularity when $15.0 < V_{max} < 24.0$ fps which can be explained consistently in light of Miles' theory since the critical layer thickness in this range is greater than 0.5 inches. This is taken to imply that the pressure sensor is constantly moving in and out of the critical layer with the passage of every wave. The effect of keeping the pressure probe in the critical layer on the recorded pressure signal can be demonstrated effectively by comparing the pressure signal in this velocity range to the pressure recorded in the same velocity range but by a pressure sensor following the water surface (shown in Fig. 9 for the same frequency wave). The sinusoidal pressure, and phase shift obtained when the pressure sensor follows the water surface at $V_{max} = 21.5$ fps and the irregular signal obtained at the same velocity when the pressure sensor is fixed in space, demonstrates conclusively the importance of letting the pressure sensor follow the water surface when the critical layer is significantly smaller than the wave height (which is often the case for moderate and high wind speeds).

Finally, Fig. 10 shows that as the maximum wind speed is increased beyond 24.0 fps, the pressure signal exhibits a periodic behavior again with a frequency equal to that of the wave. The critical layer thickness in this range is approximately 0.25 in. so that the pressure sensor (near the interface) remains outside the critical layer at all times. The pressure trace is 180 deg out-of-phase with respect to the wave and is consistent with the inviscid theory.

Based on the above discussion, the results of Wiegel and Cross [1966] can be explained consistently. Their pressure records were obtained from a static probe fixed in space above the crest of a wave having an approximate wave height of 1.0 inch. The corresponding critical layer thickness was estimated to be approximately 0.01 inch. Thus, the pressure signal is expected to be 180 deg out-of-phase with the wave as, indeed, their simultaneously recorded signals of pressure and wave height indicate. The pressure signal presented by Wiegel and Cross, however, shows a certain degree of asymmetry with respect to the wave. This can be explained

perhaps by the finiteness of amplitude of the waves above which the pressures were recorded. Such behavior has been reported by Motzfeld (1937) and Bonchkovskaya (1959) in studies of flow over fixed wavy boundaries.

CONCLUSIONS

The experimental results of this investigation are seen to be the first successful direct attempt to measure the phase shift in the pressure distribution over a train of progressive waves due to the interaction of the wave with the air boundary layer.

The necessity to make the pressure sensor follow the water surface is effectively demonstrated by comparing pressures obtained from a sensor following the water surface to pressures obtained from a pressure sensor fixed in space above the crest. The results obtained from a fixed sensor suggest that a limited verification of Miles' theory can be accomplished, even with a probe fixed in space, provided the pressure sensor remains in the critical layer.

Finally, the velocity results suggest that waves have an influence on the mean velocity distribution in air which is dependent on the wave characteristics.

ACKNOWLEDGEMENT

This work was supported under a research program sponsored by the National Science Foundation under Grants GP-2401 and GK-736 and the Fluid Dynamic Branch, Office of Naval Research, U.S. Navy, under contract Nonr-225(71), NR 062-320.

REFERENCES

- Benjamin, T. B. (1959). Shearing flow over a wavy boundary: *J. Fluid Mech.*, vol. 6, pp. 161-205.
- Bonchkouskaya, T. V. (1955). Wind flow over solid wave models: *Akademia Nauk SSR, Morskoi Gidrofizicheskii Institut*, vol. 6, pp. 98-106.
- Cohen, L. S., and Hanratty, T. S. (1965). Generation of waves in the co-current flow of air and a liquid: *A.I.Ch.E. Jour.*, vol. 11, pp. 138-144.
- Cox, C. S. (1958). Measurement of slopes of high frequency wind waves: *J. Marine Res.*, vol. 16, pp. 199-225.
- Hidy, G. and Plate, E. (1965). Wind action on water standing in a laboratory channel: Manuscript No. 66, *Nat. Cent. Atmos. Res.*, Boulder, Colorado.
- Holmes, P. (1963). Wind generation of waves: Ph. D. Thesis, College of Swansea, Univ. of Wales.
- Hsu, E. Y. (1965). A wind water-wave facility: Tech. Rep. No. 57, Dept. Civil Eng., Stanford Univ., Stanford, California.

- Jeffreys, H. (1925, 1926). On the formation of water waves by wind. Proc. Roy. Soc., Ser. A., vol. 107, pp. 189-206, and vol. 110, pp. 241-247.
- Lamb, H. (1945). Hydrodynamics, 6th ed., Dover Pubs., N. Y., Arts. 232 and 268.
- Larras, H. and Claria, W. (1960). Recherches en souffleries sur l'action relative de la houle et du vent La Houille Blanche, vol 6, pp. 647-677.
- Lighthill, M. J. (1962). Physical interpretation of mathematical theory of wave generation by wind: J Fluid Mech., vol 14, pp. 385-398.
- Longuet-Higgins, M. S. (1962). The directional spectrum of ocean waves and process of wave generation: Proc. Roy. Soc., Ser. A. vol. 265, pp. 286-315.
- Miles, J. W. (1957, 1959a, 1959b, 1961). On the generation of surface waves by shearflows. J. Fluid Mech., 1) vol. 3, pp. 185-204, 2) vol. 6, pp. 568-582, 3) vol. 6, pp. 583-598, and 4) vol. 7, pp. 433-478.
- Motzfeld, H. (1937). Die Turbulente stromungan welligen wänden: Z. Angew. Math. Mech., vol. 17, pp. 193-212.
- Phillips, O. M. (1957) On the generation of waves by turbulent wind J. Fluid Mech., vol. 2, pp. 417-445.
- Ursell, F. (1956) Wave generation by wind Surveys in Mechanics, Camb. Univ. Press, pp. 216-249.
- Wiegel, R. L. and Cross, R. H. (1966). Generation of wind waves. J. Waterways and Harbors Div., ASCE, vol. 92, pp. 1-26.
- Zagustin, K., Hsu, E. Y., Street, R. L., and Perry, B. (1966). Flow over a moving boundary in relation to wind generated waves Tech Rep. No. 60, Dept. Civil Eng., Stanford Univ., Stanford, Calif.

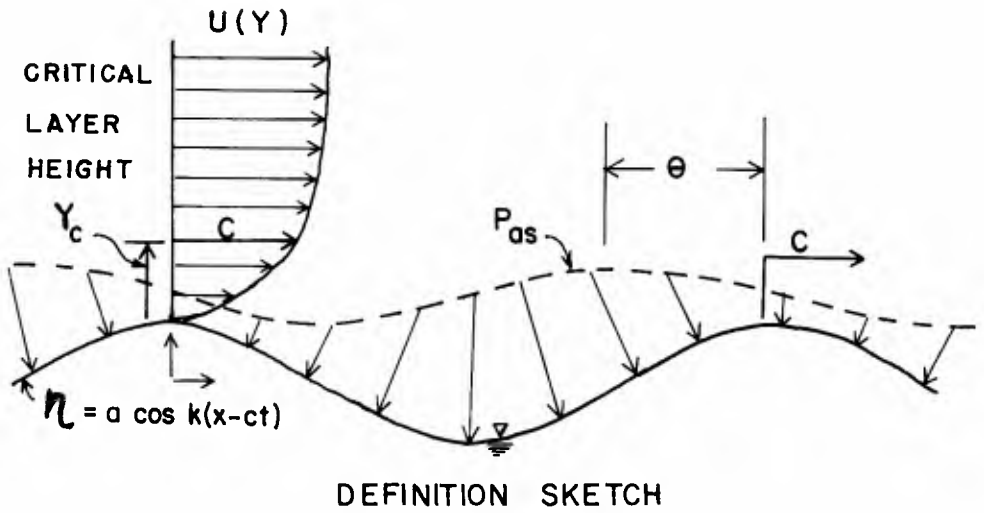
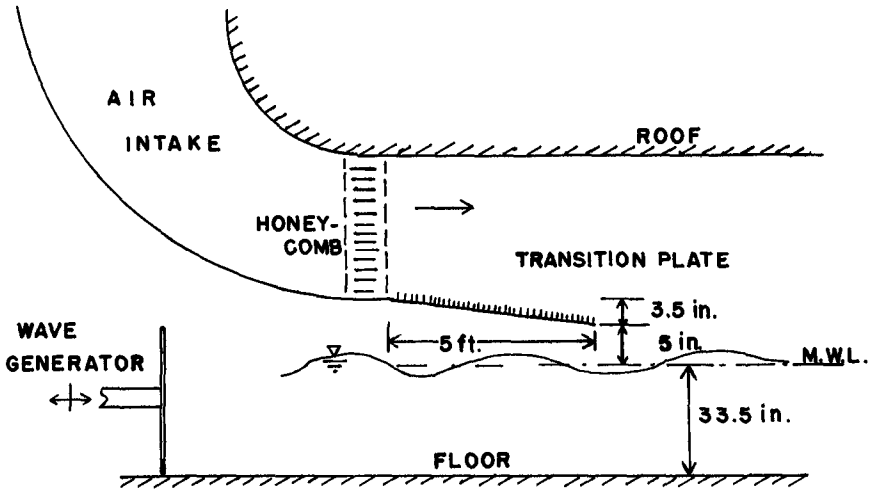


Fig. 1. Definition sketch for the air-water interface.



Fig. 2. Typical portion of the test section (Dimensions: channel cross section, 74-1/2" high x 35-1/2" wide).^{1e)}



AIR INTAKE TRANSITION PLATE

Fig. 3. Air intake to the test section and transition plate.

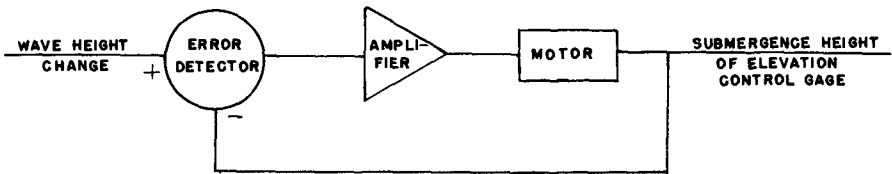


Fig. 4. Schematic diagram of electronic control of wave follower.



(a)



(b)



(c)

Fig. 5. The wave follower.

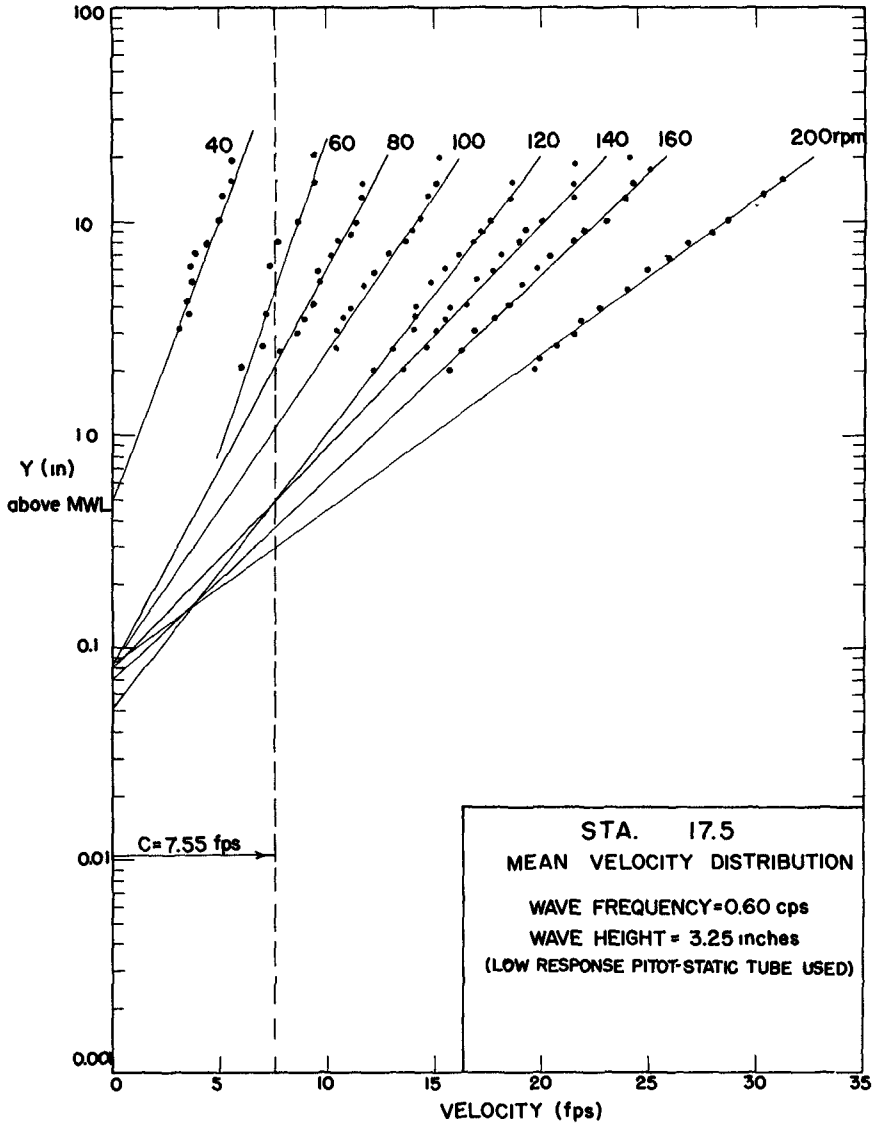


Fig. 6. Mean velocity profiles at sta 17.5 over a 0.6 cps mechanically-generated wave.

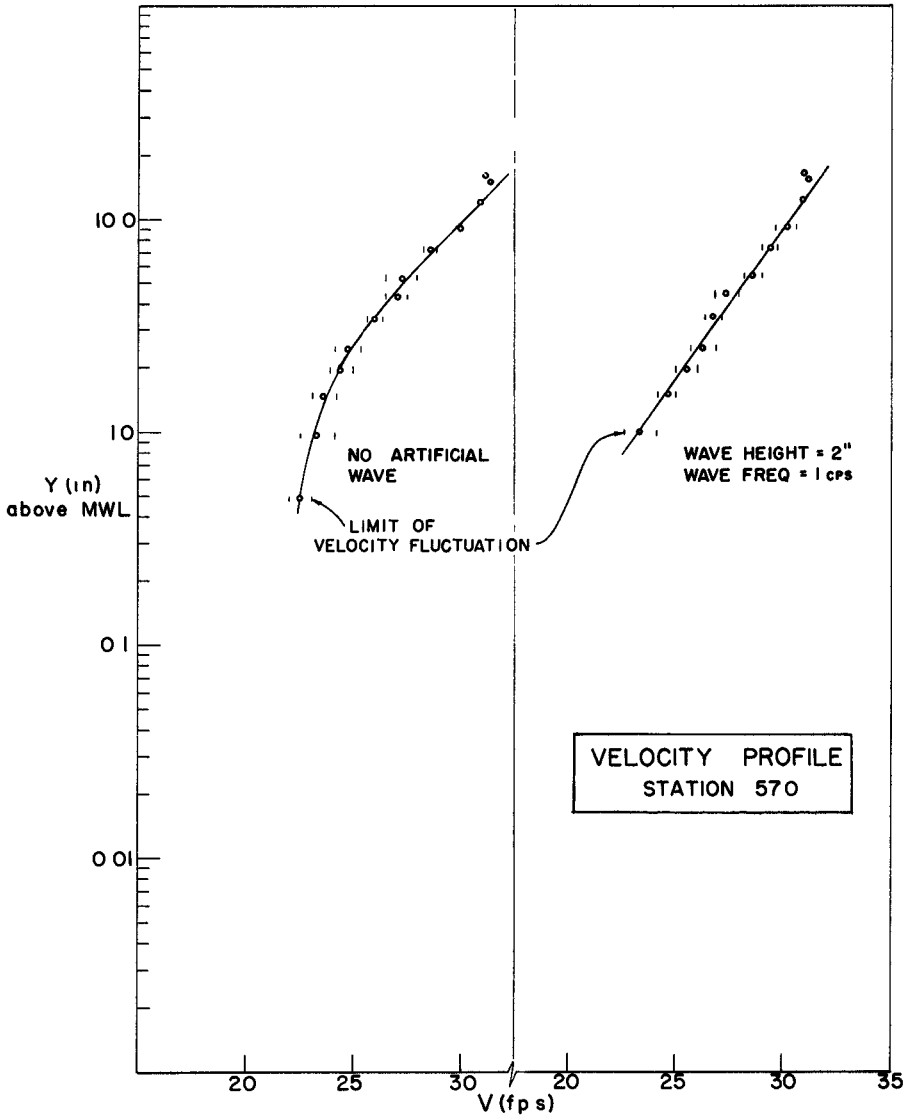


Fig. 7. Comparison of mean velocity profiles with and without mechanically-generated waves at sta 57.0.

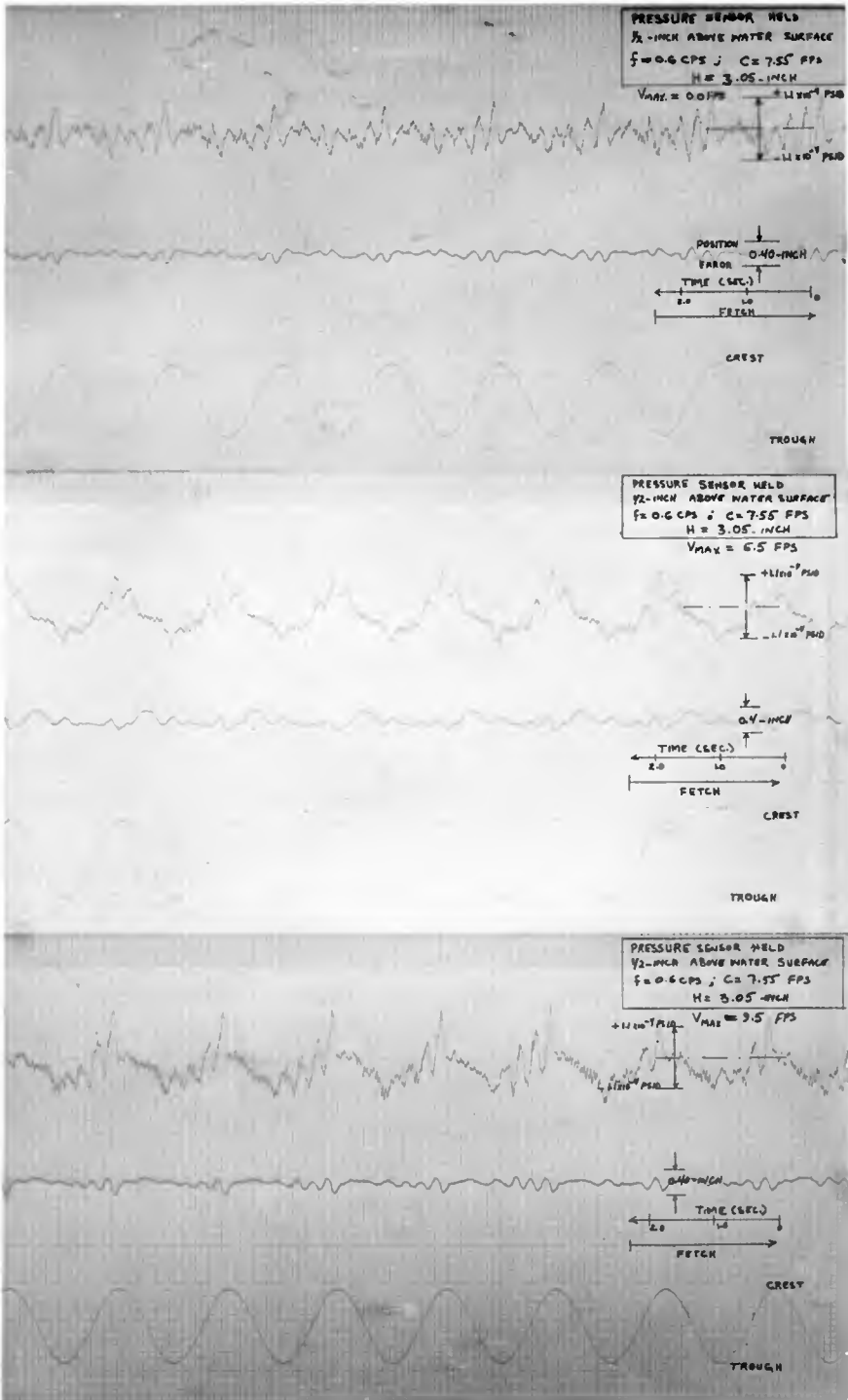


Fig. 8. Original records of pressure distribution over a 0.6 cps mechanically-generated wave having a wave height of 3.05 inches when the pressure sensor follows the water surface. Wind speeds - 0.0, 5.5, 9.5 fps.

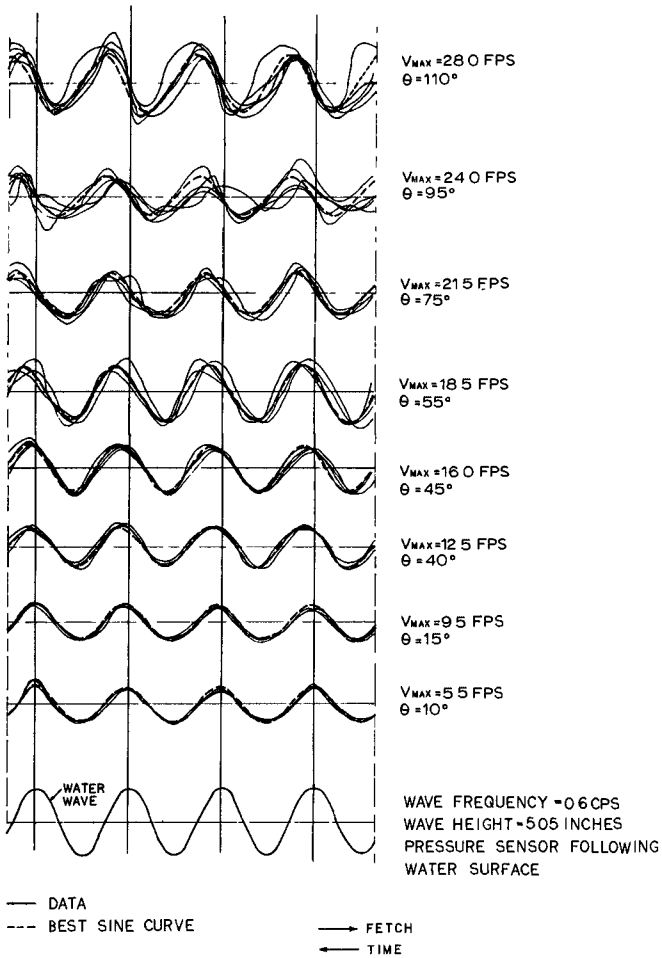


Fig. 9. Superimposed distributions of pressure over a 0.6 cps mechanically-generated wave having a wave height of 3.05 inches when the pressure sensor follows the water surface. Wind speed increases upward from 0.0 to 28.0 fps.

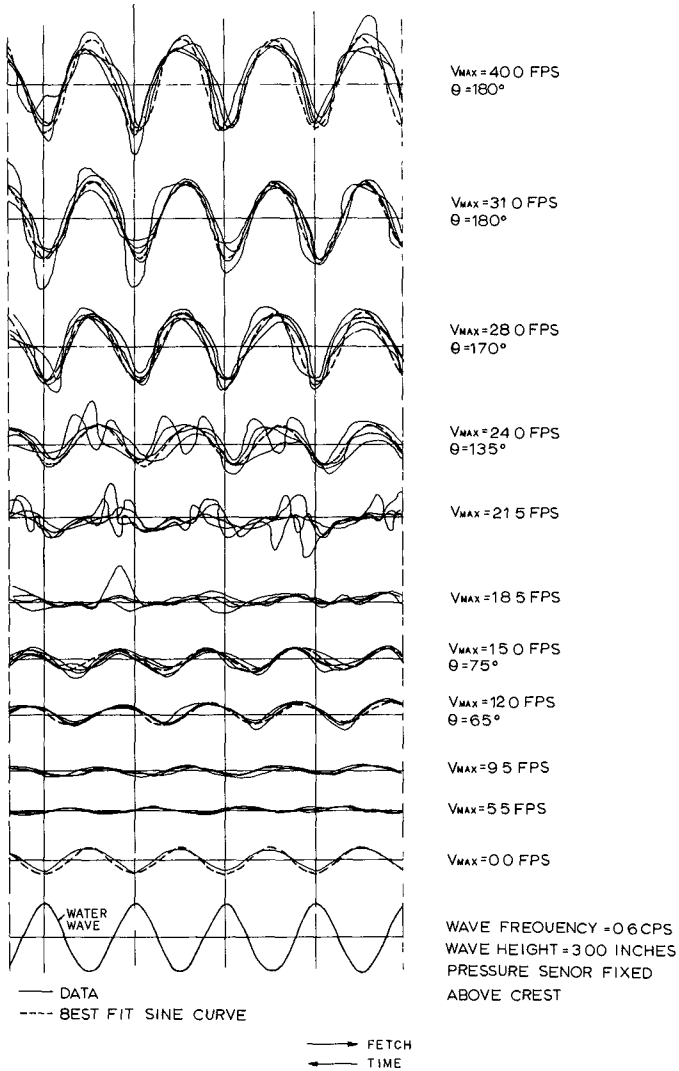


Fig. 10. Superimposed distributions of pressure over a 0.6 cps mechanically-generated wave having a wave height of 3.0 inches when the pressure sensor is fixed in space above the crest. Wind speed increases upward from 0.0 to 40.0 fps.